# Recent progress and challenges of transparent AlON ceramics

Jian WU[1,2,3], Zhuo-jian WANG[1,3], Zhi-chen HU[1,3], Xing-liang LIU[1,3],
Dun-qiang TAN[1,2], Yu DAI[1,2,3], Dong-sheng GENG[4]

1. School of Physics and Materials Science, Nanchang University, Nanchang 330031, China;
2. International Institute of Materials Innovation, Nanchang University, Nanchang 330031, China;
3. Hunan Advanced Corporation for Materials & Equipments Co., Ltd., Changsha 410118, China;
4. Beijing Advanced Innovation Center for Materials Genome Engineering, School of Materials Science and Engineering, University of Science and Technology Beijing, Beijing 100083, China

**Abstract:** The transparent AlON ceramics have attracted a growing investigation and application in the commercial and military fields, such as infrared and visible windows, domes, and transparent armors. Up to now, although great progress has been reported, such as the improved methods, new sintering additives, and fresh explored applications, a systematic and targeted summary is still lacking. In addition, there are some unsolved problems and challenges of the AlON ceramics, which hinder their commercial promotion and application. In this review, we introduce various preparation methods of AlON ceramics, including high temperature solid-state reaction, carbonization based on $Al_2O_3$, chemical vapor deposition, and sol−gel method, and thoroughly provide contrastive analysis of their advantages and disadvantages. Furthermore, we also give an insight into the transparency, sintering additives, and sintering technologies of AlON ceramics. At last, the challenges and prospects of AlON ceramics are discussed as well.

**Key words:** transparent AlON ceramics; binary $Al_2O_3$−AlN system; $Y_2O_3$ sintering additive

## 1 Introduction

Ceramics and their composites have been widely investigated for various applications due to their unique chemical and physics properties [1−7]. Among them, transparent ceramics have an extensive application in the business domain and the military industries due to their outstanding optical, physical, and mechanical properties [8−10]. Among the transparent ceramics, transparent aluminum oxynitride (AlON) ceramics have been considered as one of the most important ceramics in the domes, infrared and visible windows, and transparent armors, etc [11−13]. Compared with the single crystal sapphire, which is well-known as the hardest transparent ceramics, the polycrystalline AlON ceramics have similar characteristics on strength, hardness, and optical properties, but offer more flexibility in size and shape [14,15]. Therefore, AlON ceramics have attracted a growing investigation.

$\gamma$-AlON is a solid solution of $Al_2O_3$ and AlN [16,17]. Many methods have been explored to prepare AlON powder or AlON ceramics, such as solid-state reaction [18], carbonization method for $Al_2O_3$ [19,20], chemical vapor deposition [21], sol−gel method [22,23], and solution combustion synthesis [24]. The band gap of AlON was measured to be 6.2 eV [25]. TU et al [26] employed a first-principles density functional theory (DFT) to study the on-site preference of Al vacancy and N

atoms in $\gamma$-AlON. The band gap and bulk modulus of the $Al_{23}O_{27}N_5$ were calculated to be 3.99 eV and 200.9 GPa, respectively. Given a wide band gap together with low photon energy and high thermal stability, AlON ceramic has been explored as a phosphor matrix. As an upconversion photo-luminescence (UCPL) phosphor, AlON can be doped with various rare earth elements, such as $Eu^{2+}$ [27], $Yb^{3+}$ [28], $Tm^{3+}$ [29], and $Ce^{3+}$ [30]. Recently, the glasses based on the low-cost AlON combined with the 4-dimethyl-amino-N-methyl-4-stilbazoliumtosylate (DAST) layer [31] and a $VO_2$ thin film on the transparent AlON [32] were found to have potential application in smart windows. The ALON(5)−DAST(90)−ALON(5) outperforms industry-standard commercial window glasses with the remarks of cheapest, lightweight, and toughest [31]. Furthermore, the $Ti_6Al_4V$ was successfully prepared on the AlON ceramic through an active element brazing method, and the composite exhibited outstanding mechanical properties [33]. It should be noted that new sintering additives of $H_3BO_3$ [34] and earth elements (Sc, La, Pr, Sm, Gd, Dy, Er, and Yb) [35] were different from the conventional $Y_2O_3$, $La_2O_3$, and MgO. Although the improved methods, new sintering additives, more complex earth elements doping and fresh explored application, etc, have been extensively developed, a systematic, targeted and up-to-date summary is still lacking [11,13,36,37]. Furthermore, some unsolved problems and new challenges of the AlON ceramics hinder their commercial promotion and application. Therefore, this article takes the latest and critical review of transparent AlON ceramics in terms of preparation methods, sintering additives, sintering technologies, the challenges and development prospects.

## 2 Properties of AlON

$\gamma$-AlON has a cubic spinel structure with a space group of $Fd3m$ [38,39]. As shown in Fig. 1 [40], N and O atoms are situated at the 32e sites, and Al atoms are located at the 16d and 8a sites. Based on experimental results and theoretical calculations, the constant anion structure model of AlON could be described by the formula of $Al_{(64+x)/3}V_{(8-x)/3}O_{32-x}N_x$, where $2{\leq}x{\leq}5$ [39−42]. However, it is difficult to confirm the sensible

structural model of $\gamma$-AlON, as the local structure of N atoms and Al vacancies in $\gamma$-AlON is not clear. The properties of $\gamma$-AlON are displayed in Table 1 [14].
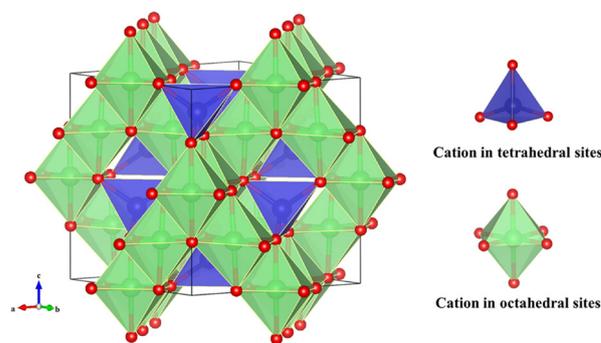


**Fig. 1** Schematic drawing of cubic spinel structure [40] (Red ball represents O/N)

**Table 1** Properties of $\gamma$-AlON [14]

| Parameter | Value |
|---|---|
| Density/(g·cm$^{-3}$) | 3.71 |
| Lattice parameter/Å | 7.947 |
| Melting point/°C | 2140 |
| Young's modulus/GPa | 323.6 |
| Shear modulus/GPa | 130.4 |
| Microhardness/GPa | 19.5 |
| Poisson ratio, $\mu$ | 0.24 |
| Bending strength/MPa | 300.1±34.5 |
| Thermal expansion/°C$^{-1}$ | $7.8\times10^{-6}$ |
| Thermal conductivity/(W·m$^{-1}$·K$^{-1}$) | 12.6 |
| Refractive index ($\Lambda$=4.0 μm)/% | 1.66 |
| Fracture toughness/(MPa·m$^{1/2}$) | 2.0 |

In 1964, the first phase diagram of binary $Al_2O_3$−AlN composition was published by LEJUS [43]. Then, MCCAULEY et al [44,45] reported a more complete phase equilibrium diagram of the pseudo-binary $Al_2O_3$−AlN composition under the flowing nitrogen at $1.013\times10^5$ Pa, as shown in Fig. 2 [44]. Besides the experimental determination, some researchers have tried to calculate the AlON stability region and the pseudo-binary $Al_2O_3$−AlN system based on the experimental data and the available thermodynamic data of the phase equilibrium diagram [36,46−49]. However, the phase segregation happening in the experiments is still unable to be modified because of the less experimental information [47].
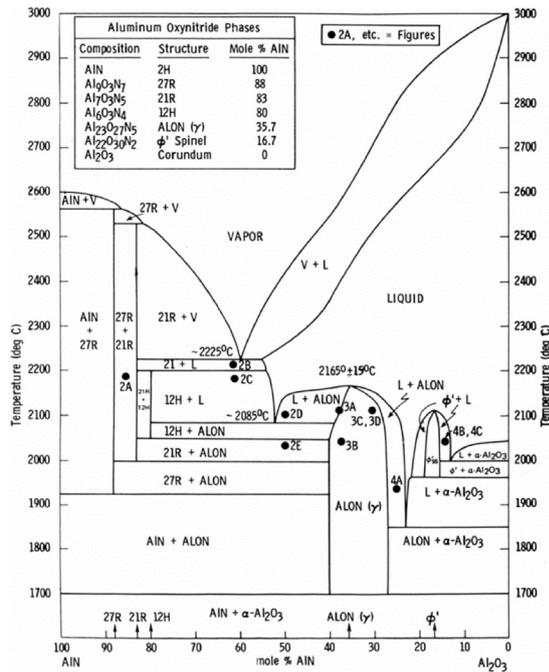
**Fig. 2** Phase diagram of pseudo-binary $Al_2O_3$−AlN composition under flowing nitrogen at $1.013 \times 10^5$ Pa [44]

## 3 Transparency of AlON

It is well known that ceramics feature grains, grain boundaries, and porosity, etc (Fig. 3) [50,51]. As mentioned before, AlON ceramics possess an isotropic cubic lattice structure, which is one of the significant reasons that they can be optically transparent. Among the light-scattering sources, the porosity is the most important factor to determine whether ceramics can be transparent or not. The minimizing porosity should be greater than 99.9% of theoretical density, and the size of pores at the grain boundaries should be smaller than the wavelength of light or should not exist. Grain boundaries are an unavoidable presence in ceramics and have a considerable impact on transparency. So, grain boundaries with high quality and grains with smaller and uniform sizes are expected to obtain high-transparency AlON ceramics. Using the sintering additives can usually eliminate the residual pores during sintering, but it will give rise to new scattering centers of light in ceramics, the secondary phase, and the inclusions. As the two important light-scattering sources, the porosity and the grain boundaries should be reduced as much as possible. SHAHBAZI et al [51] described the transparent ceramics, effective parameters on transparency, Mie theory, and Fraunhofer theory in detail.

## 4 Preparation methods

To date, many methods have been reported to prepare the AlON power or AlON ceramics, such as solid-state reaction [18,52−55], carbonization method from $Al_2O_3$ [19,56−61], chemical vapor deposition [21,62], and sol−gel method [22,63]. Most of the studies focused on the solid-state reaction of $Al_2O_3$ and AlN at a high temperature and the carbonization method for $Al_2O_3$ reduction.

### 4.1 Solid-state reaction of $Al_2O_3$ and AlN

The solid-state method is a simple and conventional approach for the preparation of many compounds. One of the greatest advantages of the solid-state reaction at a high temperature is that raw materials can be effortlessly obtained. The reaction
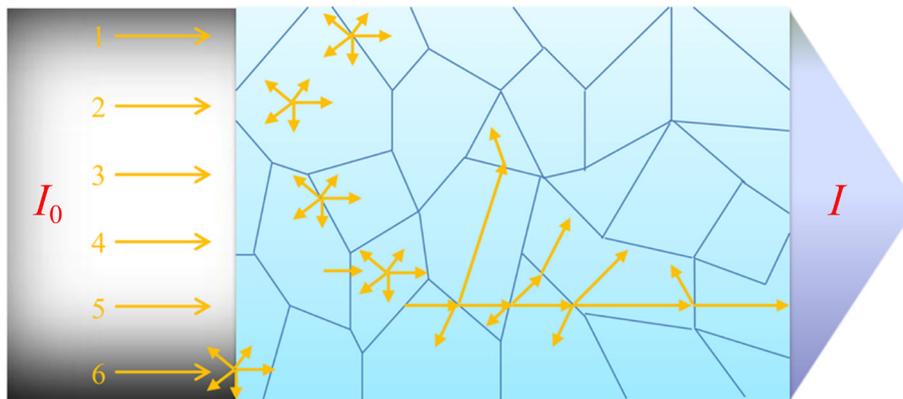


**Fig. 3** Schematic diagram of light-scattering sources in ceramics (1−6 represent grain boundaries, residual pores, secondary phase, inclusions, double refraction and surface roughness, respectively. $I_0$ and $I$ are input power intensity and output power intensity, respectively) [50,51]

of $Al_2O_3$ and AlN for AlON formation can be described as $5AlN+9Al_2O_3 \rightarrow Al_{23}O_{27}N_5$ [13,64]. The highly pure $Al_2O_3$ and AlN powers are available in the market and can be directly used to fabricate AlON powers or even the translucent AlON ceramics. The one-step preparation of the AlON ceramics can not only significantly reduce the sintering cost but also simplify the sintering process as well as easily achieve large-scale production. However, the powders may be aggregated or mixed inhomogeneously, resulting in the poor transparency of the AlON ceramics. Meanwhile, the high-purity ultrafine AlN is expensive, which increases the manufacturing cost.

As shown in Fig. 4(a), MCCAULEY and CORBIN [52] firstly prepared the translucent AlON disc and presented a refined high-temperature phase diagram of the AlON along the pseudordinary $Al_2O_3$−AlN composition joint. The liquid-phase sintering process was employed to produce transparent AlON ceramics by PATEL et al [65]. The $\alpha$-$Al_2O_3$ in the range of 27−30 mol.% was firstly mixed with AlN. Then, the mixture was pressed into pellets after ball milling. The pellets were sintered at 1950−2025 °C for 10−60 min, and part materials could form a liquid phase to promote the sintering at this stage. Next, the system temperature fell by 50−100 °C and was kept for another 8−20 h to further improve the density and transparency. CHEN et al [66] firstly synthesized a phase of pure AlON:$Ce^{3+}$ power at 1780 °C in nitrogen, then the full dense and transparent AlON:$Ce^{3+}$ ceramics were achieved by liquid-phase-assisted pressureless sintering at 1900 °C for
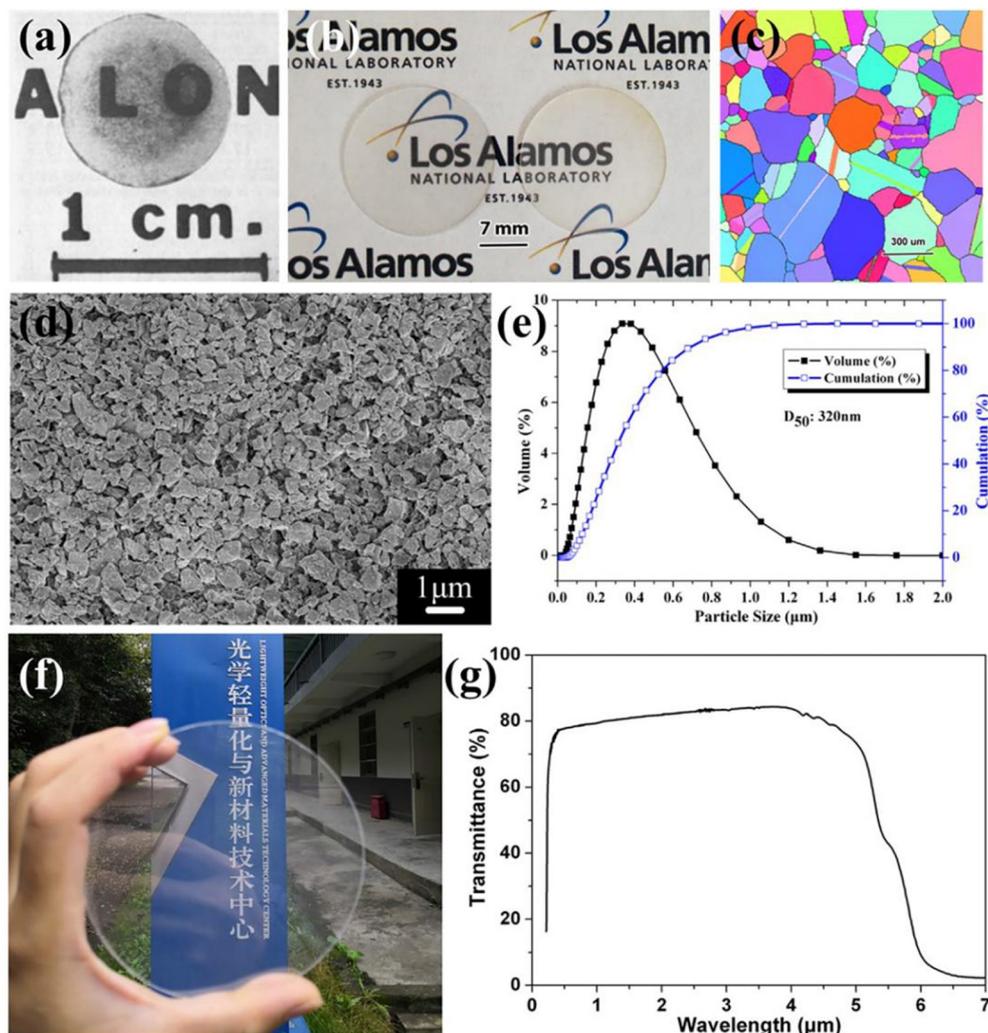


**Fig. 4** (a) First translucent AlON disc [52]; (b, c) Photograph and EBSD image of polished AlON:$Ce^{3+}_{0.005}$ disk after pressureless sintering in nitrogen at 1900 °C for 20 h, respectively [66]; (d, e) SEM image and particle size distribution of produced AlON powder after ball-milling for 24 h, respectively; (f, g) Photograph and in-line transmission spectrum of polished AlON transparent ceramic, respectively [67]

20 h (Figs. 4(a) and (b)). Besides direct synthesis of the translucent AlON ceramics by a solid-state method, LI et al [67] used $Al_2O_3$ and AlN powders as raw materials to rapidly synthesize single-phase AlON powers firstly via a solid-state method. Then, the prepared AlON powders were ground into fine AlON powders, as shown in Figs. 4(d) and (e). The transparent AlON ceramic was produced by pressureless sintering the obtained fine AlON powders, and the in-line transmittance of the AlON ceramic was as high as 84.3% ($d$100 mm × 1 mm) at 3.7 μm (Figs. 4(f) and (g)).

### 4.2 Carbonization method for $Al_2O_3$ reduction

The carbothermal reduction and nitridation (CRN) approach was firstly used to produce the compound of AlON by YAMAGUCHI and YANAGIDA in 1959 [39]. The CRN is the most used method to prepare AlON powders and then employed to produce AlON ceramics. The major advantage of this method lies in the low cost of the raw materials and the feasibility for industrial production. However, the sintering conditions are complex, and it is hard to precisely control the mole ratio of $Al_2O_3$ to C, and the AlON is easily decomposed into $Al_2O_3$ and AlN in the $N_2$ atmosphere at a high temperature. All of these might result in impure AlON powders.

JIN et al [68] firstly fabricated an $Al_2O_3$/urea-formaldehyde-resin nanocomposite precursor, which was used to produce the core-shell $Al_2O_3$/C mixture, as shown in Figs. 5(a−c). During the carbothermal nitridation process, the carbon layer on the $Al_2O_3$ particle surface was found to strongly retard the coalescence and growth of the $Al_2O_3$ particles. Finally, the transparent AlON ceramics
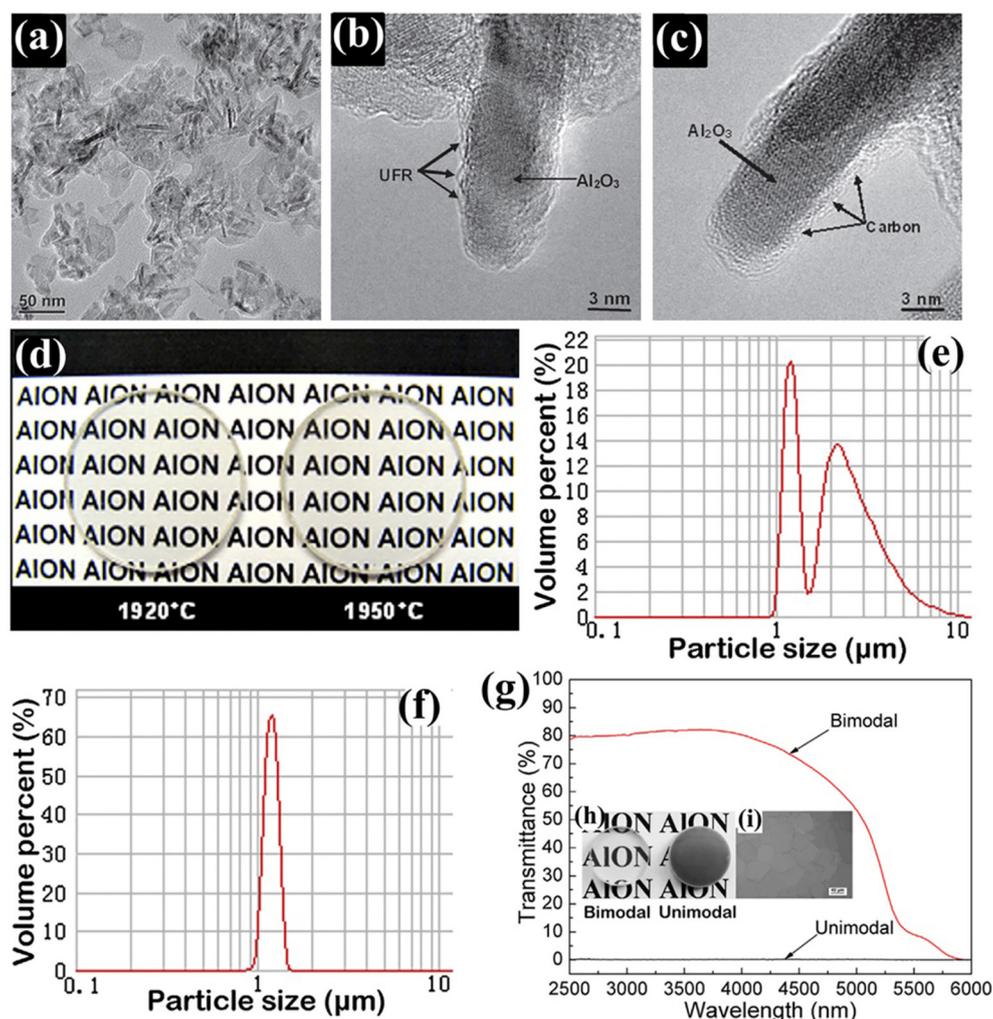


**Fig. 5** (a−c) HRTEM images of pyrolyzed $Al_2O_3$/C mixture, needle-like $Al_2O_3$/UFR particle and needle-like $Al_2O_3$/C particles, respectively; (d) Optical images of transparent AlON sintered at 1920 °C and 1950 °C [68]; (e, f) Particle size distribution of bimodal and unimodal AlON powders, respectively; (g, h) Transmittance and optical images of bimodal and unimodal AlON samples, respectively; (i) Microstructure of bimodal sample [69]

with maximum in-line transmittance above 80% at 2000 nm can be achieved by the two-step carbothermal nitridation method in nitrogen at 1950 °C for 8 h (Fig. 5(d)). SHAN et al [69] reported that both a bimodal (~1.1 μm and ~2.2 μm) and a unimodal (~1.1 μm) AlON powders could be obtained by using a ball mill of the as-prepared AlON powder via the CRN method (Figs. 5(e) and (f)). They found that the AlON powder with

bimodal particle size distribution (PSD) possesses fast densification during the sintering process, and excellent transparent AlON ceramics with up to 82.1% infrared transmittance at ~3600 nm was pressureless sintered in nitrogen at 1820 °C for 2.5 h (Fig. 5(g)).

The fine and pure γ-AlON powders were successfully prepared by YUAN et al [70] via a combinational method (Figs. 6(a) and (b)). They
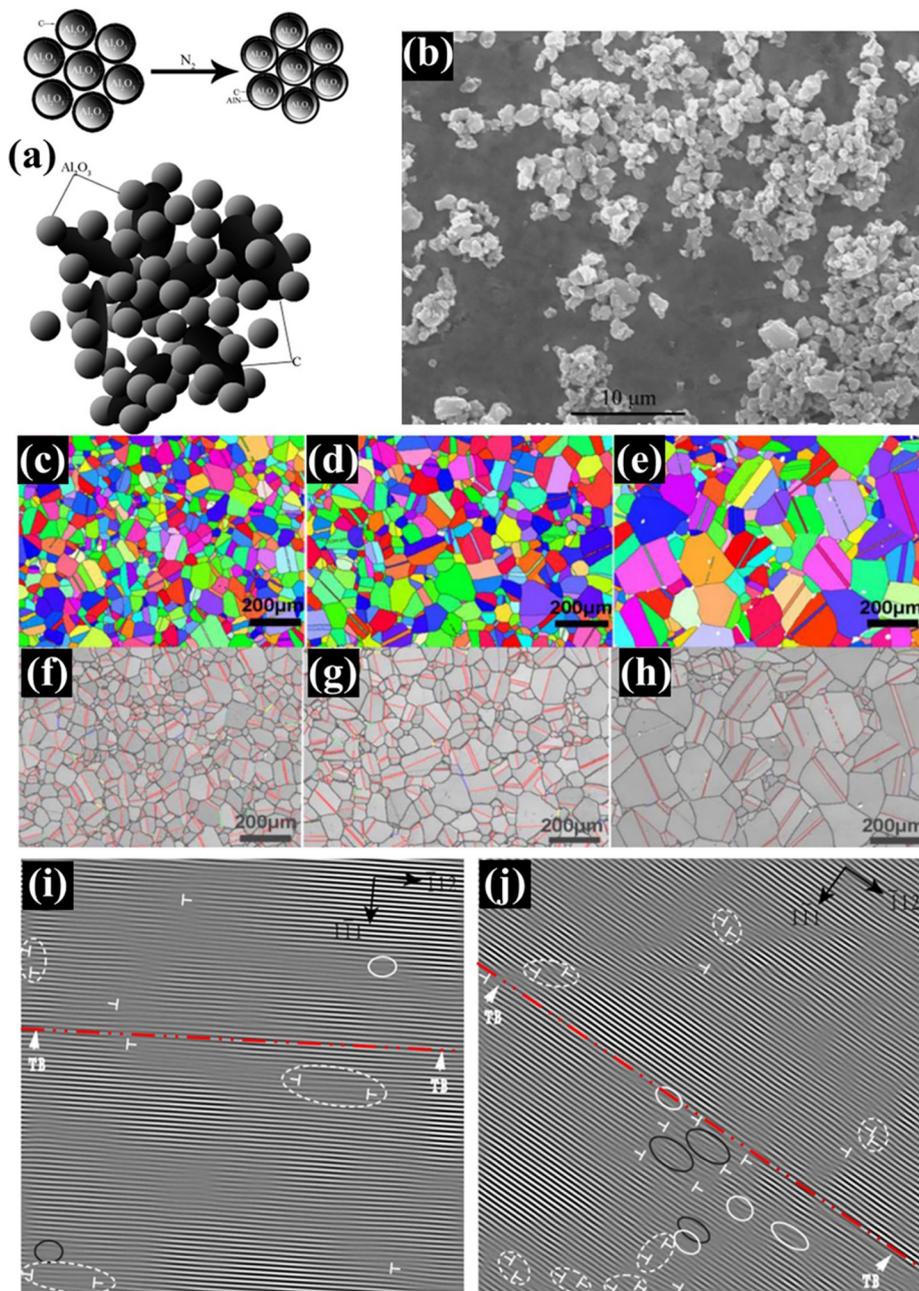


**Fig. 6** (a) Schematic diagrams for nitridation with sucrose as reducer and mixture of γ-Al$_2$O$_3$ and carbon black; (b) SEM image of γ-AlON powers [70]; (c−e) EBSD orientation maps of AlON sintered at 1880 °C for 4 h, 1950 °C for 4 h, and 1950 °C for 20 h, respectively; (f−h) Corresponding grain boundary maps of AlON sintered at 1880 °C for 4 h, 1950 °C for 4 h, and 1950 °C for 20 h, respectively with twin boundaries marked in red; (i, j) Fourier filtered HRTEM images of original AlON twin boundary region and Vickers indentation impacted twin boundary region, respectively [71]

further used the γ-AlON powders to produce AlON ceramics and studied the effect of the twin lamellas on their mechanical strength (Figs. 6(c−j)) [71]. They found that the twin lamellas and boundaries rise with the increase of the average grain size in the large-sized AlON ceramics, which provided a promising approach to enhance the transparent ceramics with large grains.

### 4.3 Other methods

Up to now, there are also other methods explored to synthesize the AlON powder or ceramics. For example, ASPAR et al [62] prepared the AlON compound using ammonia, trimethyl-aluminium, and nitrous oxide by a chemical vapor deposition (CVD) method. It was found that the temperature and pressure have a significant effect on the equilibrium compositions by modifying the quantity of CO present. IRENE et al [21] also applied the CVD method to produce $Al_xO_yN_z$ films on silicon. Importantly, the phase can be controlled by adjusting the ratio of $NH_3/CO_2$ gas and preparation temperature.

KIM et al [72] developed a low-temperature sol−gel based approach to obtain an Al-O-N system, although it may be difficult to handle the nitride precursor of hydrazine in this process. Some other nitriding agents were explored in their further investigation. KIKKAWA et al [73] fabricated AlON via ammonia nitridation of an oxide precursor, which was produced by peptizing a glycine gel with the aluminum nitrate. In addition, a plasma reactor has been designed to synthesize AlON nanopowders according to the interaction of Al powder with ammonia and air in a thermal nitrogen plasma [74]. The phase, chemical, and dispersal compositions of the prepared nano-powders are correlated with the plasma process parameters and the reactor design.

## 5 Sintering additives

To obtain high-transparency AlON ceramics, the sintering additives should be added to eliminate the residual pores during sintering, which are the scattering center of the light. Nowadays, various sintering additives for AlON, such as $Y_2O_3$, $La_2O_3$, MgO, $SiO_2$, and $CaCO_3$, have been widely investigated [67−69,75−80]. According to the types of the sintering additives, we summarized the typical transparency results of AlON ceramics with various sintering additives, as shown in Table 2. For example, SHAN et al [69] reported that the in-line transmittance of AlON ceramic (3 mm in thickness) is 82.1% at a wavelength of 3600 nm with 0.5 wt.% $Y_2O_3$. $SiO_2$ was firstly employed as the sintering additive for the AlON ceramic (Fig. 7(b)) [76]. They found that the in-line transmittance of AlON ceramic is up to 86% (3.5 mm in thickness) at 2000 nm and is not sensitive to the additive concentration with 0.15−0.55 wt.% $SiO_2$. Some researchers used two types of sintering additives to produce high-transparent AlON ceramics. WANG et al [81] used 0.12wt.%$Y_2O_3$−0.09wt.%$La_2O_3$ as co-additives for the AlON ceramics, obtaining a transmittance of 80.3% (2 mm in thickness) at 400 nm (Fig. 7(a)). They reported that $Y^{3+}$ and $La^{3+}$ have a synergistic effect on the grain growth with

**Table 2** Transparency results of AlON ceramics with various sintering additives

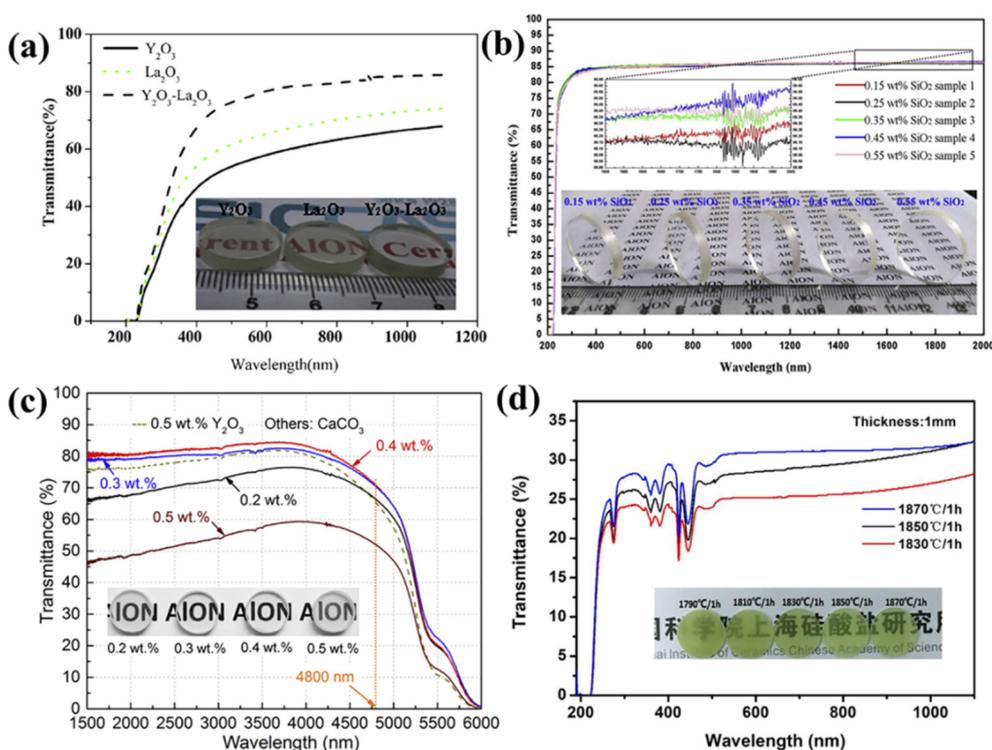| Type of sintering additive | $Y_2O_3$ content/ wt.% | $La_2O_3$ content/ wt.% | MgO content/ wt.% | $SiO_2$ content/ wt.% | $CaCO_3$ content/ wt.% | Wavelength/ nm | Transmittance/ % | Thickness/ mm | Ref. |
|---|---|---|---|---|---|---|---|---|---|
| | | | | 0.15−0.55 | | 2000 | 86 | 3.5 | [76] |
| | | | | | 0.4 | 3700 | 85 | 3 | [79] |
| 1 | 0.5 | | | | | 3700 | 84.3 | 1 | [67] |
| | 0.5 | | | | | 3600 | 82.1 | 3 | [69] |
| | | 0.02 | | | | 1100 | 74.6 | 4.2 | [75] |
| | 0.12 | 0.09 | | | | 400 | 80.3 | 2 | [80] |
| 2 | 0.4 | | 0.25 | | | 2000 | 86.1 | 1 | [78] |
| | 0.05 | | 0.2 | | | 2000 | 84 | 1.5 | [77] |
| 3 | 0.08 | 0.025 | 0.1 | | | 1100 | 81 | 1 | [68] |

**Fig. 7** (a, b) In-line transmittance spectra of AlON ceramics with 0.08 wt.% $Y_2O_3$, 0.02 wt.% $La_2O_3$, and 0.08 wt.% $Y_2O_3$−0.02 wt.% $La_2O_3$ (a) [75], concentration of $SiO_2$ (b) [76], 0.2−0.5 wt.% $CaCO_3$ and 0.5 wt.% $Y_2O_3$ (c) [79] and 0.1 wt.% MnO (d) [81]

the $Y^{3+}$ improving the mobility of grain boundary and promoting the grain growth while the $La^{3+}$ inhibited the grain growth. JIN et al [68] sintered AlON ceramics employing three types of sintering additives without pressure, composited by 0.1 wt.% MgO, 0.08 wt.% $Y_2O_3$, and 0.025 wt.% $La_2O_3$, and achieved a transmittance of 81% (1 mm in thickness) at 1100 nm. Recently, $Y_2O_3$−$La_2O_3$−MnO as a composite sintering additive to fabricate the transparent AlON ceramics was investigated by WANG et al [81] (Fig. 7(d)). The solubility limits of the sintering additives in AlON were studied by MILLER and KAPLAN [82] using wavelength-dispersive spectroscopy mounted on a scanning electron microscope. They found that the solubility limits of La, Y, and Mg in AlON at 1870 °C were $(498\pm82)\times10^{-6}$, $(1775\pm128)\times10^{-6}$, and $>4000\times10^{-6}$, respectively.

In addition to the conventional sintering additives of $Y_2O_3$, $La_2O_3$, and MgO, new sintering additives of $H_3BO_3$ based ternary composite [34] and earth elements [35] were also investigated. As illustrated in Figs. 8(a) and (b), various rare earth elements (Sc, La, Pr, Sm, Gd, Dy, Er, and Yb) were systematically explored as a sintering additive for

transparent AlON ceramics, respectively. It was found that the AlON ceramics with 0.1 wt.% Pr-nitrate presented the highest transmittance of ~80% by two-step pressureless sintering (Fig. 8(c)), indicating that the rare earth elements can be a promising alternative sintering additive. More recently, using a $Y_2O_3$−$MgAl_2O_4$−$H_3BO_3$ as the co-sintering additive, YANG et al [34] obtained AlON ceramic with a transmittance of 81% (4 mm in thickness) at 600 nm by one-step reactive sintering when the $H_3BO_3$ content was 0.12 wt.% (Fig. 8(d)).

# 6 Sintering technologies

Before sintering, green pellets of the AlON powders are usually formed by a dry process, including a uniaxial press under pressure and cold isostatic press, or by a wet process, including gel-casting [8,63,83]. Many sintering technologies have been explored to prepare AlON ceramics, such as pressureless sintering [56,58,67,68,77,79], vacuum sintering [65], hot-press [84], microwave sintering [85,86], spark plasma sintering [87−89] and hot isostatic pressing [75,76,78,90,91]. The

advantages and disadvantages of the common preparation methods of AlON ceramic are shown in Table 3.

Pressureless sintering is the most traditional sintering technology and is cost-effective for the

mass production of AlON ceramics with various sizes and shapes. However, high sintering temperature, long sintering time, and sintering additives are generally required to obtain the high-transparent AlON ceramics. LI et al [67] reported a
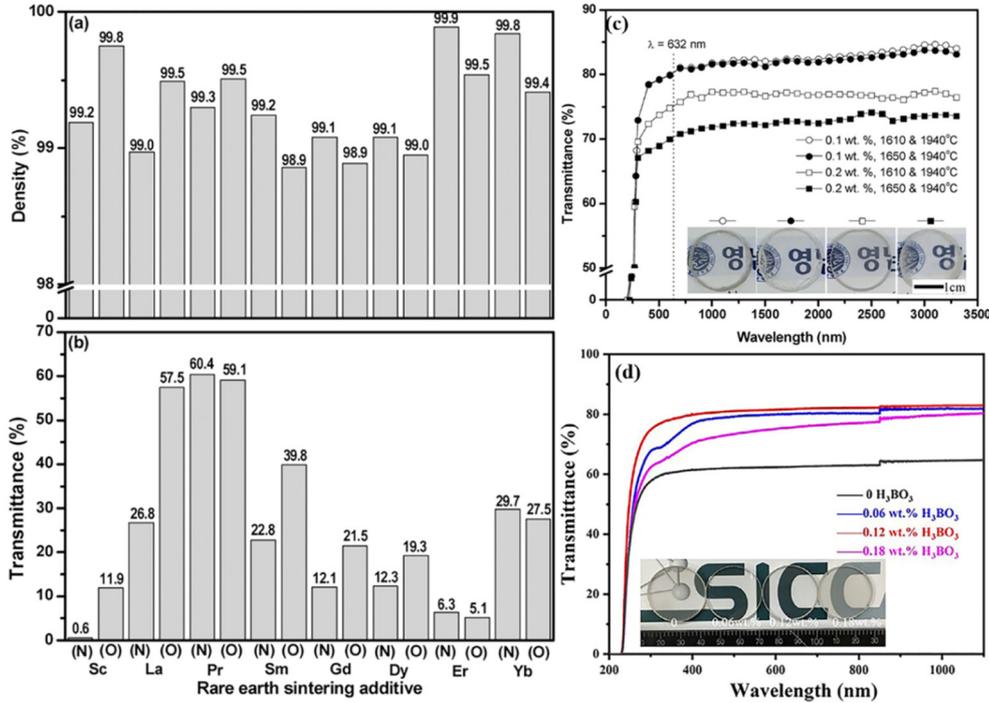


**Fig. 8** Comparison of density (a) and transmittance (b) of prepared AlON doped with different rare earth element [35], and transmittance of AlON with Pr-nitrate (c) [35] and $0.1wt.\%Y_2O_3−0.4wt.\%MgAl_2O_4−xwt.\%H_3BO_3$ (d) [34] as additives

**Table 3** Advantages and disadvantages of common preparation methods of AlON ceramic

| Preparation method | Advantage | Disadvantage |
|---|---|---|
| Pressureless sintering | Simple process, suitable to prepare large and complex samples, low requirement on equipment, and high output | Low energy efficiency, and long sintering time |
| Vacuum sintering | Simple process, suitable to prepare large and complex samples, low requirement on equipment, and high output | Low energy efficiency, and long sintering time |
| Spark plasma sintering | High energy efficiency, low sintering temperature, short sintering time, and cost-saving | Not suitable to prepare large and complex samples, high requirement on equipment, and low output |
| Microwave sintering | High energy efficiency, low sintering temperature, short sintering time, and cost-saving | Not suitable to prepare large and complex samples, high requirement on equipment, and low output |
| Hot-press sintering | High transmittance, high density, and low residual pores | Not suitable to prepare large and complex samples, high requirement on equipment, low output, complex process, and high cost |
| Hot isostatic pressing | High transmittance, high density, and low residual pores | Not suitable to prepare large and complex samples, High requirement on equipment, low output, complex process, and high cost |

large number of transparent AlON ceramics with dimensions of $d$100 mm × 1 mm by pressureless sintering at 1950 °C for 12 h under flowing $N_2$ atmosphere in a graphite furnace. The in-line transmittance of the AlON ceramic (1 mm in thickness) is 84.3% at 3.7 μm wavelength with 0.5 wt.% $Y_2O_3$. Vacuum sintering is an effective sintering technology to eliminate gas from ceramics [92]. PATEL et al [65] used high-purity $Al_2O_3$ and AlN powers as the raw materials to fabricate the translucent AlON ceramics at 2000 °C for 8 h and 32 MPa of pressure under hot-press, following at 1900 °C for more than 8 h in a vacuum. Hot-press (HP) sintering can be employed to apply axial pressure to accelerate the movement of powers and make the green pellet fully dense at a relatively low temperature. But the HP sintering is not suitable to prepare large and complex samples, and the production is high cost, and impurities and defects can be inevitably introduced. A post-annealing process is needed to remove carbon contamination [8]. TAKEDA and HOSAKA [84] obtained transparent $\lambda$-AlON ceramic at 1900 °C for 1 h and 20 MPa of pressure under hot-press. Microwave sintering possesses high energy efficiency, cost-saving, low sintering temperature, strengthened reaction, and sintering rate. In the microwave process, the converted microwave energy

can heat within the sample volume itself. CHENG et al [85] presented that the AlON sintered at 1800 °C for 1 h during the microwave process has a total transmission of 60%. Spark plasma sintering (SPS), also called the pulsed electric current sintering, can realize dense transparent ceramics with fine grains due to its short sintering time and low temperature with the aid of pulsed DC under pressure. So, the grain growth can be reduced. SHAN et al [87] produced high-transparent AlON ceramics by SPS at the low temperature of 1600 °C and the fast heating rates of 50−250 °C/min under the pressure of 60 MPa. The maximum transmittance of the as-obtained AlON ceramics (1.4 mm in thickness) is 80.6%.

Hot isostatic pressing (HIP) is the most powerful sintering technology to achieve the maximum density and high-end optical transmitting ceramics by ultimately reducing residual pores in ceramics [8,11,93,94]. During high-temperature sintering, the HIP equipment can be applied by isostatic gas pressure. Figure 9 shows the schematic diagram of the microstructure model for pore elimination by the HIP [8,95]. Normally, it is significantly difficult to eliminate residual pores by other sintering technologies. An additional HIP procedure is required to eliminate the residual pores and increase the density and transmittance very close to the theoretical value.
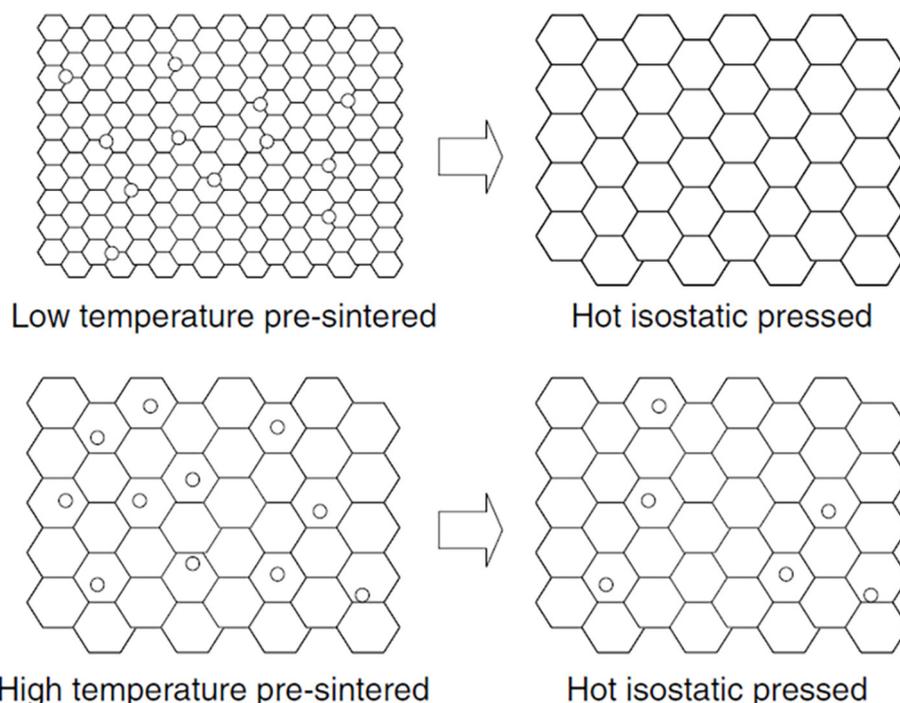


Low temperature pre-sintered       Hot isostatic pressed

High temperature pre-sintered      Hot isostatic pressed

**Fig. 9** Schematic diagram of microstructure model for pore elimination by hot isostatic pressing [95]

# 7 Conclusions and future directions

The transparent AlON ceramic possesses excellent optical, physical, and mechanical characteristics. These advantages make it useful in infrared and visible windows, domes and transparent armors, semi-conductor processing applications, and military aircraft lenses, etc. Compared with the single crystal sapphire, the polycrystalline AlON ceramics have similar characteristics on strength, hardness, and optical properties, but present more flexibility in size and shape. The article takes the latest and critical review of the AlON ceramics from the preparation methods, sintering additives, sintering technologies, the challenges and development prospects.

Although extensive research on the material has been carried out, there are still many problems and challenges. Firstly, with the development of national defense technology, the high cost and small size of the as-prepared AlON ceramics hinder their commercial promotion and application. Therefore, how to prepare high-transparent AlON ceramic with large-scale and low cost is the most important challenge. Secondly, the manufacturing technology should have a simple process, and the resulting products should be at an affordable price. For example, the HP/HIP technology is considered an efficient sintering method for the fabrication of AlON ceramics with good optical quality. However, it is not suitable to produce large-scale AlON ceramics, and the production costs are high. In addition, it is difficult to fabricate large-scale green bodies with complex shapes due to the possible cracks that may appear during the drying process. Last but not the list, owing to the high hardness of the AlON ceramics, it is difficult to grind and polish, resulting in high requirements on the equipment and high cost.

Therefore, the future trend is to prepare high-transparent AlON ceramic with large-scale and low cost through simple technology and processes. For example, employing continuous production to replace traditional bath production toward the synthesis of the AlON power can increase productivity effectively, thus making costs down. Besides, the pressureless sintering technology is a good choice to reduce the cost and fabricate the large-scale sample. In addition, more concerns should be put on the exploring of the low cost but high effectively sintering additives. According to the above issues, further efforts should be made to solve the mentioned problems and challenges to realize the development prospect and widen the commercial application of the AlON ceramics.

## Acknowledgments

## References

[1]  DUAN Chuan-cheng, KEE R J, ZHU Hua-yang, KARAKAYA C, CHEN Ya-chao, RICOTE S, JARRY A, CRUMLIN E J, HOOK D, BRAUN R, SULLIVAN N P, O'HAYRE R. Highly durable, coking and sulfur tolerant, fuel-flexible protonic ceramic fuel cells [J]. Nature, 2018, 557: 217−222.

[2]  ZHU Yun-tong, GONZALEZ-ROSILLO J C, BALAISH M, HOOD Z D, KIM K J, RUPP J L M. Lithium-film ceramics for solid-state lithionic devices [J]. Nature Reviews Materials, 2020, 6: 313−331.

[3]  LIU Yang, YU Yang, YIN Chen-yi, ZHENG Liang, ZHENG Peng, BAI Wang-feng, LI Li-li, WEN Fei, ZHANG Yang. Achieving remarkable piezoelectric activity in Sb−Mn co-modified $CaBi_4Ti_4O_{15}$ piezoelectric ceramics [J]. Transactions of Nonferrous Metals Society of China, 2021, 31: 2442−2453.

[4]  TAN Yan-ni, CHEN Wen-juan, WEI Wei, HUANG Qian-li, HE Xiang. Rubidium-modified bioactive glass−ceramics with hydroxyapatite crystals for bone regeneration [J]. Transactions of Nonferrous Metals Society of China, 2021, 31: 521−532.

[5]  YANG Jie, XU Long-hua, WU Hou-qin, JIN Jiao. Preparation and properties of porous ceramics from spodumene flotation tailings by low-temperature sintering [J]. Transactions of Nonferrous Metals Society of China, 2021, 31: 2797−2811.

[6]  ZHONG Xin, ZHANG Chen, CHEN Fang-xu, TANG Zhu-ming, JIAN Gang. Dielectric properties and relaxor ferroelectric behavior of $(1-y)Ba(Zr_{0.1}Ti_{0.9})O_3-yBa(Zn_{1/3}Nb_{2/3})O_3$ ceramics [J]. Transactions of Nonferrous Metals Society of China, 2020, 30: 756−764.

[7]  ZOU Ke, ZOU Jian-peng, DENG Chun-ming, LIU Min, LIU Xue-zhang, ZHAO Rui-min, LI Shun-hua, ZHU Ren-bo, GAO Di. Preparation and properties of supersonic atmospheric plasma sprayed $TiB_2$−SiC coating [J]. Transactions of Nonferrous Metals Society of China, 2021, 31: 243−254.

[8]  JUNG W K, MA Ho Jin, KIM H N, KIM D K. Transparent

ceramics for visible/IR windows: Processing, materials and characterization [J]. Korean Journal of Materials Research, 2018, 28: 551−563.

[9] KIM W, VILLALOBOS G R, BAKER C, FRANTZ J A, SHAW B, BAYYA S S, SADOWSKI B, AGGARWAL I D, HUNT M, SANGHERA J. Ceramic windows and gain media for high-energy lasers [J]. Optical Engineering, 2012, 52: 1−8.

[10] KRELL A, KLIMKE J, HUTZLER T. Transparent compact ceramics: Inherent physical issues [J]. Optical Materials, 2009, 31: 1144−1150.

[11] LIU Xue-jian, CHEN Feng, ZHANG Fang, ZHANG Hai-long, ZHANG Zong-hao, WANG Jun, WANG Shi-wei, HUANG Zheng-ren. Hard transparent AlON ceramic for visible/IR windows [J]. International Journal of Refractory Metals and Hard Materials, 2013, 39: 38−43.

[12] RUAN Guo-zhi, XU Hai-sen, ZHANG Zhi-hui, YIN Ming-qiang, XU Guo-gang, ZHAN Xiao-yuan. New method of synthesizing aluminum oxynitride spinel powders [J]. Journal of the American Ceramic Society, 2013, 96: 1706−1708.

[13] CORBIN N D. Aluminum oxynitride spinel: A review [J]. Journal of the European Ceramic Society, 1989, 5: 143−154.

[14] HARTNETT T M, BERNSTEIN S D, MAGUIRE E A, TUSTISON R W. Optical properties of ALON (aluminum oxynitride) [J]. Infrared Physics & Technology, 1998, 39: 203−211.

[15] MAGUIRE E A, RAWSON J K, TUSTISON R W. Aluminum oxynitride's resistance to impact and erosion [J]. Proceedings of SPIE—The International Society for Optical Engineering, 1994, 2286: 26−32.

[16] LONG G, FOSTER L M. Crystal phases in the system $Al_2O_3$−AlN [J]. Journal of the American Ceramic Society, 1961, 44: 255−258.

[17] WILLEMS H X, METSELAAR R, HELMHOLDT R B, PETERSEN K K. Neutron diffraction of $\gamma$-aluminium oxynitride [J]. Journal of Materials Science Letters, 1993, 12: 1470−1472.

[18] MAGHSOUDIPOUR A, BAHREVAR M A, HEINRICH J G, MOZTARZADEH F. Reaction sintering of AlN−AlON composites [J]. Journal of the European Ceramic Society, 2005, 25: 1067−1072.

[19] RAFANIELLO W, CUTLER I B. Preparation of sinterable cubic aluminum oxynitride by the carbothermal nitridation of aluminum oxide [J]. Journal of the American Ceramic Society, 1981, 64: 128.

[20] SHAN Ying-chun, HOU Guan-bing, SUN Xian-nian, HAN Xiao-guang, HONG Chang-qing, XU Jiu-jun, LI Jiang-tao. One-step carbothermal reduction and nitridation (CRN) for fast fabrication of fine and single phase AlON powder by using hydrothermal synthesized $\alpha$-$Al_2O_3$/C mixture [J]. Ceramics International, 2021, 47: 18012−18019.

[21] IRENE E A, SILVESTRI V J, WOOLHOUSE G R. Some properties of chemically vapor deposited films of $Al_xO_yN_z$ on silicon [J]. Journal of Electronic Materials, 1975, 4: 409−427.

[22] NADERI B B, ALIZADEH A. Preparation of single phase AlON powders aided by the nitridation of sol−gel-derived nanoparticles [J]. Ceramics International, 2019, 45: 7537−7543.

[23] NADERI B B, ALIZADEH A. Development of a new sol−gel route for the preparation of aluminum oxynitride nano-powders [J]. Ceramics International, 2020, 46: 913−920.

[24] ZHANG Yi-ming, WU Hao-yang, QIN Ming-li, WANG Yue-long, ZHANG Zhi-rui, ZHANG De-yin, JIA Bao-rui, QU Xuan-hui. Rapid synthesis of AlON powders by nitriding combustion synthesis precursor [J]. Ceramics International, 2021, 47: 23590−23596.

[25] FRENCH R H. Electronic band structure of $Al_2O_3$, with comparison to AlON and AlN [J]. Journal of the American Ceramic Society, 1990, 73: 477−489.

[26] TU Bing-tian, WANG Hao, LIU Xiao, WANG Wei-min, FU Zheng-yi. First-principles study on site preference of aluminum vacancy and nitrogen atoms in $\gamma$-AlON [J]. Journal of the American Ceramic Society, 2013, 96: 1937−1943.

[27] ZHANG Fang, CHEN Shi, CHEN Jin-fang, ZHANG Hai-long, LI Jun, LIU Xue-jian, WANG Shi-wei. Characterization and luminescence properties of AlON:$Eu^{2+}$ phosphor for white-emitting-diode illumination [J]. Journal of Applied Physics, 2012, 111: 083532−083535.

[28] SU Ming-yi, ZHOU You-fu, WANG Kun, HUANG De-cai, XU Wen-tao, CAO Yong-ge. Effect of $Yb^{3+}$ concentration on upconversion luminescence of AlON:$Er^{3+}$ phosphors [J]. Journal of Rare Earths, 2015, 33: 227−230.

[29] ZHANG Fang, AN Li-qiong, LIU Xue-jian, ZHOU Guo-hong, YUAN Xian-yang, WANG Shi-wei. Upconversion luminescence in $\gamma$-AlON:$Yb^{3+}$, $Tm^{3+}$ ceramic phosphors [J]. Journal of the American Ceramic Society, 2009, 92: 1888−1890.

[30] SI Jia-yong, WANG Le, LIU Li-hong, YI Wei, CAI Ge-mei, TAKEDA T, FUNAHASHI S, HIROSAKI N, XIE Rong-jun. Structure, luminescence and energy transfer in $Ce^{3+}$ and $Mn^{2+}$ codoped $\gamma$-AlON phosphors [J]. Journal of Materials Chemistry C, 2019, 7: 733−742.

[31] CHOWDHARY A K, SIKDAR D. Design of electrotunable all-weather smart windows [J]. Solar Energy Materials and Solar Cells, 2021, 222: 110921−110930.

[32] PENG Bo, SHI Qi-wu, HUANG Wan-xia, WANG Shan-shan, QI Jian-qi, LU Tie-cheng. Transparent AlON ceramic combined with $VO_2$ thin film for infrared and terahertz smart window [J]. Ceramics International, 2018, 44: 13674−13680.

[33] LI Chun, ZHANG Kai-ping, MAO Xiao-jian, SI Xiao-qing, LAN Bo, LIU Zhan-Guo, HUANG Yong-xian, QI Jun-lei, FENG Ji-cai, CAO Jian. Microstructure and mechanical properties of the AlON/$Ti_6Al_4V$ active element brazing joint [J]. Materials Science and Engineering: A, 2020, 793: 139859−139867.

[34] YANG Shui-xian, LI Jian-min, GUO Hao, MAO Xiao-jian, TIAN Run, ZHANG Jian, WANG Shi-wei. Reactive sintered highly transparent AlON ceramics with $Y_2O_3$−$MgAl_2O_4$−$H_3BO_3$ ternary additive [J]. Journal of the American Ceramic Society, 2021, 104: 4304−4308.

[35] TSABIT A M, KIM M D, YOON D H. Effects of various rare-earth additives on the sintering and transmittance of $\gamma$-AlON [J]. Journal of the European Ceramic Society, 2020, 40: 3235−3243.

[36] MCCAULEY J W, PATEL P, CHEN Ming-wei, GILDE G, STRASSBURGER E, PALIWAL B, RAMESH K T, DANDEKAR D P. AlON: A brief history of its emergence and evolution [J]. Journal of the European Ceramic Society, 2009, 29: 223−236.

[37] YANG J, CONG Y, LING J R, XU W T, ZHANG Y, ZHOU Y F, HONG M C. Preparation of transparent AlON from powers synthesized by novel CRN method [J]. Journal of the European Ceramic Society, 2022, 42: 935−943.

[38] WU Jian, GUO Pan, MI Rui, LIU Xi-chuan, ZHANG Hui, MEI Jun, LIU Hao, LAU Woon-ming, LIU Li-min. Ultrathin $NiCo_2O_4$ nanosheets grown on three-dimensional interwoven nitrogen-doped carbon nanotubes as binder-free electrodes for high-performance supercapacitors [J]. Journal of Materials Chemistry A, 2015, 3: 15331−15338.

[39] YAMAGUCHI G, YANAGIDA H. Study on the reductive spinel—A new spinel formula $AlN−Al_2O_3$ instead of the previous one $Al_3O_4$ [J]. Bulletin of the Chemical Society of Japan, 1959, 32: 1264−1265.

[40] CLAYTON J D. A nonlinear thermomechanical model of spinel ceramics applied to aluminum oxynitride (AlON) [J]. Journal of Applied Mechanics, 2010, 78: 011013−011011.

[41] TABARY P, SERVANT C. Crystalline and microstructure study of the $AlN−Al_2O_3$ section in the Al−N−O system. I: Polytypes and $\gamma$-AlON spinel phase [J]. Journal of Applied Crystallography, 1999, 32: 241−252.

[42] OKEKE O U, LOWTHER J E. Elastic constants of oxynitride aluminum spinel phases [J]. Chemical Physics Letters, 2010, 494: 323−325.

[43] LEJUS A. Formation at high temperature of nonstoichiometric spinels and of derived phases in several oxide systems based on alumina and in the system alumina−aluminum nitride [J]. Revue Internationale des Hautes Temperatures et des Refractaires, 1964, 1: 53−95.

[44] MCCAULEY J W, CORBIN N D. High temperature reactions and microstructures in the $Al_2O_3−AlN$ system [C]// Progress in Nitrogen Ceramics. Dordrecht: Springer, 1983: 111−118.

[45] MCCAULEY J W, KRISHNAN K M, RAI R, THOMAS G, ZANGVILL A, DOSER R W, CORBIN N D. Anion controlled microstructures in the $Al_2O_3−AlN$ system [C]// Ceramic microstructures'86. Boston: Springer, 1987: 577−590.

[46] TABARY P, SERVANT C. Thermodynamic reassessment of the $AlN−Al_2O_3$ system [J]. Calphad, 1998, 22: 179−201.

[47] QIU Cai-an, METSELAAR R. Phase relations in the aluminum carbide–aluminum nitride–aluminum oxide system [J]. Journal of the American Ceramic Society, 1997, 80: 2013−2020.

[48] DUMITRESCU L, SUNDMAN B. A thermodynamic reassessment of the Si−Al−O−N system [J]. Journal of the European Ceramic Society, 1995, 15: 239−247.

[49] KAUFMAN L. Calculation of quasi binary and quasiternary oxynitride systems−III [J]. Calphad, 1979, 3: 275−291.

[50] KOOMEN M, TOUSEY R, SCOLNIK R. The spherical aberration of the eye [J]. Journal of the Optical Society of America, 1949, 39: 370−376.

[51] SHAHBAZI H, TATAEI M, ENAYATI M H, SHAFEIEY A, MALEKABADI M A. Structure−transmittance relation-

ship in transparent ceramics [J]. Journal of Alloys and Compounds, 2019, 785: 260−285.

[52] MCCAULEY J W, CORBIN N D. Phase relations and reaction sintering of transparent cubic aluminum oxynitride spinel (AlON) [J]. Journal of the American Ceramic Society, 1979, 62: 476−479.

[53] KIM Y W, PARK H C, LEE Y B, OH K D, STEVENS R. Reaction sintering and microstructural development in the system $Al_2O_3−AlN$ [J]. Journal of the European Ceramic Society, 2001, 21: 2383−2391.

[54] LI Xi-bao, LU Jin-shan, FENG Zhi-jun. Microstructural characteristics and oxidation behavior of $Y_2O_3$-doped $\gamma$-AlON [J]. Journal of Materials Science, 2015, 50: 7097−7103.

[55] BANDYOPADHYAY S, RIXECKER G, ALDINGER F, PAL S, MUKHERJEE K, MAITI H S. Effect of reaction parameters on $\gamma$-AlON formation from $Al_2O_3$ and AlN [J]. Journal of the American Ceramic Society, 2002, 85: 1010−1012.

[56] SHAN Ying-chun, ZHANG Zhao-hui, SUN Xian-nian, XU Jiu-jun, QIN Qing-hua, LI Jiang-tao. Further experimental investigation on fast densification mechanism of bimodal powder during pressureless sintering of transparent AlON ceramics [J]. Ceramics International, 2017, 43: 8195−8201.

[57] LIU Qiang, JIANG Nan, LI Jiang, SUN Kun, PAN Yu-bai, GUO Jing-kun. Highly transparent AlON ceramics sintered from powder synthesized by carbothermal reduction nitridation [J]. Ceramics International, 2016, 42: 8290−8295.

[58] SHAN Ying-chun, XU Jian-xin, WANG Guang, SUN Xian-nian, LIU Guang-hua, XU Jiu-jun, LI Jiang-tao. A fast pressureless sintering method for transparent AlON ceramics by using a bimodal particle size distribution powder [J]. Ceramics International, 2015, 41: 3992−3998.

[59] SABAGHI V, DAVAR F, TAHERIAN M H. Ultrasonic-assisted preparation of AlON from alumina/carbon core−shell nanoparticle [J]. Ceramics International, 2019, 45: 3350− 3358.

[60] WANG Ying-ying, LI Qing-gang, HUANG Shi-feng, CHENG Xin, HOU Peng-kun, WANG Yong-chen, CHEN Guan-liang, YI Shan-ling. Preparation and properties of AlON powders [J]. Ceramics International, 2018, 44: 471−476.

[61] ZHENG Jie, FORSLUND B. Carbothermal synthesis of aluminium oxynitride (AlON) powder: Influence of starting materials and synthesis parameters [J]. Journal of the European Ceramic Society, 1995, 15: 1087−1100.

[62] ASPAR B, ARMAS B, COMBESCURE C, THENEGAL D. Organometallic chemical vapour deposition in the Al−O−N system [J]. Journal of the European Ceramic Society, 1991, 8: 251−256.

[63] WANG Jun, ZHANG Fang, CHEN Feng, ZHANG Hai-long, TIAN Run, DONG Man-jiang, LIU Juan, ZHANG Zhao, ZHANG Jian, WANG Shi-wei, RIEDEL R. Fabrication of aluminum oxynitride ($\gamma$-AlON) transparent ceramics with modified gelcasting [J]. Journal of the American Ceramic Society, 2014, 97: 1353−1355.

[64] YAWEI L I, NAN L I, YUAN R Z. The formation and stability of $\gamma$-aluminium oxynitride spinel in the carbothermal reduction and reaction sintering processes [J]. Journal of Materials Science, 1997, 32: 979−982.

[65] PATEL P J, GILDER G, MCCAULEY J W. Transient liquid phase reactive sintering of aluminum oxynitride. US Patent: 7045091 B1[P]. 2006−05−16.

[66] CHEN Ching-fong, YANG Pin, KING G, TEGTMEIER E L, SETLUR A. Processing of transparent polycrystalline AlON:Ce$^{3+}$ scintillators [J]. Journal of the American Ceramic Society, 2016, 99: 424−430.

[67] LI Hai-long, MIN Pan, SONG Ning, ZHANG Ai-fang, ZHOU Jia-jun, XIAN Hao, LIU Hong, FANG Jing-zhong. Rapid synthesis of AlON powders by low temperature solid-state reaction [J]. Ceramics International, 2019, 45: 8188−8194.

[68] JIN Xi-hai, GAO Lian, SUN Jing, LIU Yang-qiao, GUI Lin-hua, KLEEBE H J. Highly transparent AlON pressurelessly sintered from powder synthesized by a novel carbothermal nitridation method [J]. Journal of the American Ceramic Society, 2012, 95: 2801−2807.

[69] SHAN Ying-chun, ZHANG Zhao-hui, SUN Xian-nian, XU Jiu-jun, QIN Qin-ghua, LI Jiang-tao. Fast densification mechanism of bimodal powder during pressureless sintering of transparent AlON ceramics [J]. Journal of the European Ceramic Society, 2016, 36: 671−678.

[70] YUAN Xin-yang, LIU Xue-jian, ZHANG Fang, WANG Shi-wei. Synthesis of γ-AlON powders by a combinational method of carbothermal reduction and solid-state reaction [J]. Journal of the American Ceramic Society, 2010, 93: 22−24.

[71] GUO Hui-lu, ZHANG Jian, MAO Xiao-jian, ZHANG Fang, SUN Feng, CHEN Feng, WANG Jun, TIAN Run, LIU Juan, WANG Shi-wei. Strengthening mechanism of twin lamellas in transparent AlON ceramics [J]. Journal of the European Ceramic Society, 2018, 38: 3235−3239.

[72] KIM J Y, SRIRAM M A, MCMICHAEL P H, KUMTA P N, PHILLIPS B L, RISBUD S H. New molecular precursors from the reaction of hydrazine and aluminum alkoxide for the synthesis of powders in the Al−O−N system [J]. The Journal of Physical Chemistry B, 1997, 101: 4689−4696.

[73] KIKKAWA S, HATTA N, TAKEDA T. Preparation of aluminum oxynitride by nitridation of a precursor derived from aluminum–glycine gel and the effects of the presence of europium [J]. Journal of the American Ceramic Society, 2008, 91: 924−928.

[74] SAMOKHIN A V, ASTASHOV A G, ALEKSEEV N V, SINAYSKY M A, TSVETKOV Y V. Synthesis of aluminum oxynitride nanopowders in a plasma reactor with a confined jet flow [J]. Inorganic Materials: Applied Research, 2018, 9: 393−398.

[75] CHEN Feng, ZHANG Fang, WANG Jun, ZHANG Hai-long, TIAN Run, ZHANG Zhao, WANG Shi-wei. Hot isostatic pressing of transparent AlON ceramics with Y$_2$O$_3$/La$_2$O$_3$ additives [J]. Journal of Alloys and Compounds, 2015, 650: 753−757.

[76] FENG Zhao, QI Jian-qi, GUO Xiao-feng, WANG Yue-zhong, CAO Xiu-xia, YU Yin, MENG Chuan-min, LU Tie-cheng. A new and highly active sintering additive: SiO$_2$ for highly-transparent AlON ceramic [J]. Journal of Alloys and Compounds, 2019, 787: 254−259.

[77] SHAN Ying-chun, SUN Xian-nian, REN Bing-lin, WU Hao-kai, WEI Xia-lu, OLEVSKY E A, XU Jiu-jun, LI Jiang-tao. Pressureless sintering of highly transparent AlON ceramics with CaCO$_3$ doping [J]. Scripta Materialia, 2018, 157: 148−151.

[78] GUO Hui-lu, MAO Xiao-jian, ZHANG Jian, TIAN Run, WANG Shi-wei. Densification of AlON ceramics doped with Y$_2$O$_3$−La$_2$O$_3$−MnO additives at lower sintering temperature [J]. Ceramics International, 2019, 45: 5080−5086.

[79] FENG Zhao, QI Jian-qi, HUANG Xu, GUO Xiao-feng, YU Yin, CAO Xiu-xia, WANG Yue-zhong, WU Di, MENG Chuan-min, LU Tie-cheng. Planetary ball-milling of AlON powder for highly transparent ceramics [J]. Journal of the American Ceramic Society, 2019, 102: 2377−2389.

[80] JIANG Nan, LIU Qiang, XIE Teng-fei, MA Peng, KOU Hua-min, PAN Yu-bai, LI Jiang. Fabrication of highly transparent AlON ceramics by hot isostatic pressing post-treatment [J]. Journal of the European Ceramic Society, 2017, 37: 4213−4216.

[81] WANG Jun, ZHANG Fang, CHEN Feng, ZHANG Jian, ZHANG Hai-long, TIAN Run, WANG Zheng-juan, LIU Juan, ZHANG Zhao, CHEN Shi, WANG Shi-wei. Effect of Y$_2$O$_3$ and La$_3$O$_3$ on the sinterability of γ-AlON transparent ceramics [J]. Journal of the European Ceramic Society, 2015, 35: 23−28.

[82] MILLER L, KAPLAN W D. Solubility limits of La and Y in aluminum oxynitride at 1870 °C [J]. Journal of the American Ceramic Society, 2008, 91: 1693−1696.

[83] WILLEMS H X, HENDRIX M M R M, DE W G, METSELAAR R. Thermodynamics of AlON II: Phase relations [J]. Journal of the European Ceramic Society, 1992, 10: 339−346.

[84] TAKEDA K, HOSAKA T. Characteristics of new raw materials AlON for refractories [J]. Interceram, 1989, 38: 18−22.

[85] CHENG Ji-ping, AGRAWAL D, ZHANG Yun-jin, ROY R. Microwave reactive sintering to fully transparent aluminum oxynitride (AlON) ceramics [J]. Journal of Materials Science Letters, 2001, 20: 77−79.

[86] CHENG Ji-ping, AGRAWAL D, ROY R. Microwave synthesis of aluminum oxynitride (AlON) [J]. Journal of Materials Science Letters, 1999, 18: 1989−1990.

[87] SHAN Ying-chun, WEI Xia-lu, SUN Xian-nian, TORRESANI E, OLEVSKY E A, XU Jiu-jun. Effect of heating rate on properties of transparent aluminum oxynitride sintered by spark plasma sintering [J]. Journal of the American Ceramic Society, 2019, 102: 662−673.

[88] SHAN Ying-chun, WEI Xia-lu, SUN Xian-nian, XU Jiu-jun, QIN Qing-hua, OLEVSKY E A. Highly infrared transparent spark plasma sintered AlON ceramics [J]. Journal of Materials Research, 2017, 32: 3279−3285.

[89] KAMALI S, MOHEBI M M, TAHERIAN M H, SABAGHI V. Highly transparent AlON fabricated via SPS synthesized by Al$_2$O$_3$/C core–shell starting powder and CRN method [J]. International Journal of Applied Ceramic Technology, 2021, 18: 724−738.

[90] LIU Li-hong, ZHANG Chen-ning, TAKAHASHI K, NISHIMURA T, SEGAWA H, HIROSAKI N, XIE Rong-jun. Uniform and fine Mg−γ-AlON powders prepared from MgAl$_2$O$_4$: A promising precursor material for highly-transparent Mg−γ-AlON ceramics [J]. Journal of the European Ceramic Society, 2019, 39: 928−933.

[91] LI Jian-min, ZHANG Bu-hao, TIAN Run, MAO Xiao-jian, ZHANG Jian, WANG Shi-wei. Hot isostatic pressing of transparent AlON ceramics assisted by dissolution of gas inclusions [J]. Journal of the European Ceramic Society, 2021, 41: 4327−4336.

[92] HUANG Yi-hua, JIANG Dong-liang, ZHANG Jing-xian, LIN Qing-ling, HUANG Zheng-ren. Sintering of transparent yttria ceramics in oxygen atmosphere [J]. Journal of the American Ceramic Society, 2010, 93: 2964−2967.

[93] TSUKUMA K, YAMASHITA I, KUSUNOSE T. Transparent 8 mol.% $Y_2O_3$−$ZrO_2$(8Y) ceramics [J]. Journal of the American Ceramic Society, 2008, 91: 813−818.

[94] ZHANG Wei, LU Tie-cheng, MA Ben-yuan, WEI Nian, LU Zhong-wen, LI Feng, GUAN Yong-bing, CHEN Xing-tao, LIU Wei, QI Lu. Improvement of optical properties of Nd:YAG transparent ceramics by post-annealing and post hot isostatic pressing [J]. Optical Materials, 2013, 35: 2405−2410.

[95] TANG Fei, CAO Yong-ge, HUANG Ji-quan, LIU Hua-gang, GUO Wang, WANG Wen-chao. Fabrication and laser behavior of composite Yb:YAG ceramic [J]. Journal of the American Ceramic Society, 2012, 95: 56−69.

# 透明 AlON 陶瓷的发展现状和挑战

吴 建 [1,2,3]，王卓健 [1,3]，胡智臣 [1,3]，刘兴亮 [1,3]，谭敦强 [1,2]，戴 煜 [1,2,3]，耿东生 [4]

1. 南昌大学 物理与材料学院，南昌 330031；

2. 南昌大学 国际材料创新研究院，南昌 330031；

3. 湖南顶立科技有限公司，长沙 410118；

4. 北京科技大学 材料科学与工程学院 北京材料基因工程高精尖创新中心，北京 100083

摘 要：氮氧化铝透明陶瓷是备受关注的材料，广泛应用于商业和军事领域，如红外和可见光窗口、透明装甲等方面。最近几年，氮氧化铝透明陶瓷得到了快速发展，出现新的制备方法、新的烧结助剂及新的应用领域。然而，目前还没有系统的、最新的相关综述。此外，氮氧化铝透明陶瓷还存在一些未解决的问题和新的挑战，严重阻碍其商业化应用。因此，本文作者全面介绍氮氧化铝陶瓷的制备方法，包括高温固相反应法、氧化铝还原氮化法、化学气相沉积法和溶胶凝胶等方法，并对这些制备方法的优缺点进行比较分析。此外，系统地总结烧结助剂和烧结工艺对氮氧化铝透明陶瓷透光性的影响。最后，对氮氧化铝透明陶瓷面临的挑战和发展趋势进行讨论和展望。

关键词：透明氮氧化铝陶瓷；$Al_2O_3$−AlN 二元体系；氧化钇烧结助剂

**(Edited by Wei-ping CHEN)**